Direct Observation of the Structure of Global Alfvén Eigenmodes in a Tokamak Plasma

T. E. Evans, P. M. Valanju, J. F. Benesch, Roger D. Bengtson, Y.-M. Li, S. M. Mahajan, M. E. Oakes, D. W. Ross, X.-Z. Wang, and J. G. Watkins
University of Texas at Austin, Austin, Texas 78712

and

C. M. Surko
AT&T Bell Laboratories, Murray Hill, New Jersey 07974
(Received 30 April 1984)

We present the first direct observation of the structure of a driven global Alfvén eigenmode in a tokamak plasma using CO_2 laser interferometry.

PACS numbers: 52.35.–g, 52.40.Db, 52.50.Gj

The properties of Alfvén waves in hot, magnetically confined plasmas are quite unlike those in homogeneous media. Despite their significance for the interpretation of both laboratory and astrophysical phenomena, experimental studies of these waves have been limited principally to the determination of the cavity eigenmode frequencies or parallel phase velocities. With the development of long confinement times in fusion experiments, laser interferometry to measure density fluctuations, and a theoretical understanding of the density fluctuations associated with Alfvén waves, it has now become possible to investigate their spatial structure.

We report the first such investigation,[1,2] which identifies and determines the structure of global Alfvén eigenmodes (GAE). These modes are particular manifestations of the effects of magnetic confinement on the Alfvén waves. Because of their relatively weak damping, the GAE can be excited to high amplitudes with an external antenna and have been previously observed as resonances in the plasma loading resistance.[3] They make up the low-frequency part of the stable discrete spectrum of magnetohydrodynamics.[4,5] They owe their existence entirely to plasma inhomogeneities, i.e., to the coupling between the shear and compressional modes brought about by gradients in the equilibrium current and density. Rediscovered as broadened resonances in calculations based on kinetic theory,[6] the GAE have been further studied, both analytically and numerically, as candidates for the heating of fusion plasmas.[7-11]

To model the GAE in a tokamak, we assume a cylindrical plasma of length $2\pi R$. The characteristic frequencies of the GAE are denoted by ω_{lm}, where l and m are the axial (toroidal) and azimuthal (poloidal) mode numbers, respectively. The plasma has axial magnetic field $B_0\hat{z}$ and current density $J_0(r)$, which determines the poloidal field $B_\theta(r)$, and hence the safety factor $q(r) \equiv rB_0/RB_\theta$. The wave number parallel to the field is $k_\parallel(r) = (-l + m/q)/R$, and the shear Alfvén frequency is defined by $\omega_A(r) \equiv k_\parallel v_A$, where $v_A(r) = B_0/(\mu_0 n m_{\rm eff})^{1/2}$, $n = n(r)$ is the plasma density, and $m_{\rm eff}$ is an effective mass which depends on the impurity concentration. To include finite-ion-gyrofrequency corrections, we use the same mass, taking $\omega_{ci} = eB_0/m_{\rm eff}$.

The characteristic frequencies of the GAE lie below the threshold of the spatial Alfvén-cyclotron resonance or the Alfvén continuum, defined by $\omega^2(1-\omega^2/\omega_{ci}^2) = \omega_A^2$.[12] That is, for these modes, l and m have opposite signs so that $k_\parallel$ is nonzero and $\omega_{lm}^2(1-\omega_{lm}^2/\omega_{ci}^2)^{-1} - \omega_A^2 < 0$ everywhere in the plasma. For each l,m there is an infinite sequence of eigenmodes, which may be denoted by a radial mode number. We omit this label here and consider only the lowest frequency or fundamental mode. The other modes tend to merge into the continuum as a result of damping from kinetic effects. For the mode numbers of interest, we may define $\omega_{A0}^2 \equiv \min[\omega_A^2(r)] = \omega_A^2(r_0)$, where $r_0 \neq 0$. Then, an approximate expression for the fundamental frequency is obtained by exanding about r_0 and solving the resulting equations variationally.[9] The result is

$$\omega_{lm}^2 = \frac{(1-\epsilon r_0^2/m^2L^2)\omega_{A0}^2}{1+(1-\epsilon r_0^2/m^2L^2)\omega_{A0}^2/\omega_{ci}^2}, \tag{1}$$

where $\epsilon = g - \frac{1}{4} - (g - \frac{1}{2})^{1/2}$, $L^{-2} \equiv (1/\omega_A^2) \times (d^2\omega_A/dr^2)|_{r=r_0}$, and g is a function of order unity which depends linearly upon the gradients of the density, q profile, and ω_{A0}/ω_{ci}. The precise frequency, ω_{lm}, is sensitive to the plasma profiles, and because of the ω/ω_{ci} terms (where ω is the driving frequency), $\omega_{l,m} \neq \omega_{-l,-m}$. To determine the damping rate and the density fluctuations, it is essential to use kinetic theory to calculate the parallel electron dynamics. The collisionless wave-particle resonance (Landau damping) is typically the dominant dissipative mechanism. In the numerical calculations,[6] the GAE appear as high-Q resonances just below the Alfvén continuum. Global modes with $l > 0, m < 0$ are dominant. Their peak loading resistance and density fluctuation amplitude are larger than those of $l < 0, m > 0$ modes and those in the continua of all four modes $(\pm l, \pm m)$.

The experiments were performed on the PRETEXT tokamak, with $R = 53$ cm, $r_a = 14$ cm, $B_0 = 7.5$–10 kG, $I_p = 20$–50 kA, $T_e = 200$–400 eV, $\bar{n}_e = (4$–$20) \times 10^{12}$ cm^{-3}, and discharge lengths of 20–100 msec. Alfvén waves are driven by two stainless-steel one-quarter-turn toroidal antennas located 180° apart toroidally and 1 cm radially inward from the vacuum vessel wall at the equatorial plane. The antennas are covered with an insulating coating and do not have Faraday shields. A resonant circuit matches the low impedance of the antenna to the 5-Ω transmission line driven by an amplifier at 2.1 MHz. The loading of the antenna is measured from the decrease in the quality factor Q of the low-loss resonant antenna-matchbox circuit[13] by sweeping the driver frequency around the resonance at low power (< 100 W).

Plasma density fluctuations driven by the antenna current are measured with a CO_2-laser interferometer system which has its detection circuitry electrically referenced to the rf antenna current through a high-frequency lock-in amplifier. The lock-in time constant of each phase-quadratured output was typically 0.3 ms. This provides a large signal-to-noise level for high-power rf operation and insures that only driven density oscillations (denoted by $\tilde{n}$) are detected. Experimentally it is found that a minimum current of 50 A in a single antenna is required to induce detectable density fluctuations. The interferometer is sensitive to wavelengths greater than the beam diameter (0.8 cm) since, for shorter wavelengths, the scattered light does not intercept the detector. The detected signal is a measure of the line integral of the amplitude and phase of density fluctuations, $\tilde{\Delta} = (2\pi/\lambda n_c)\int \tilde{n}(y)\,dy$, where $\lambda = 10.6\ \mu$m and $n_c \simeq 10^{19}$ cm^{-3} is the cutoff density. The integral extends over a region of overlap between the laser beam and plasma. We scan the plasma from shot to shot at a fixed toroidal location.

We demonstrate the GAE mode-identification technique in Figs. 1 and 2 for impedance and interferometer signals. Figure 1(a) shows the typical time behavior of the plasma density and current during a 30-ms portion of the rf pulse. Using measured data from these parameters and Eq. (1) we compute the GAE resonant frequency normalized by the rf frequency (ω_{lm}/ω). Figures 1(c) and 2(c) show plots of ω_{lm}/ω for several choices of l and m.

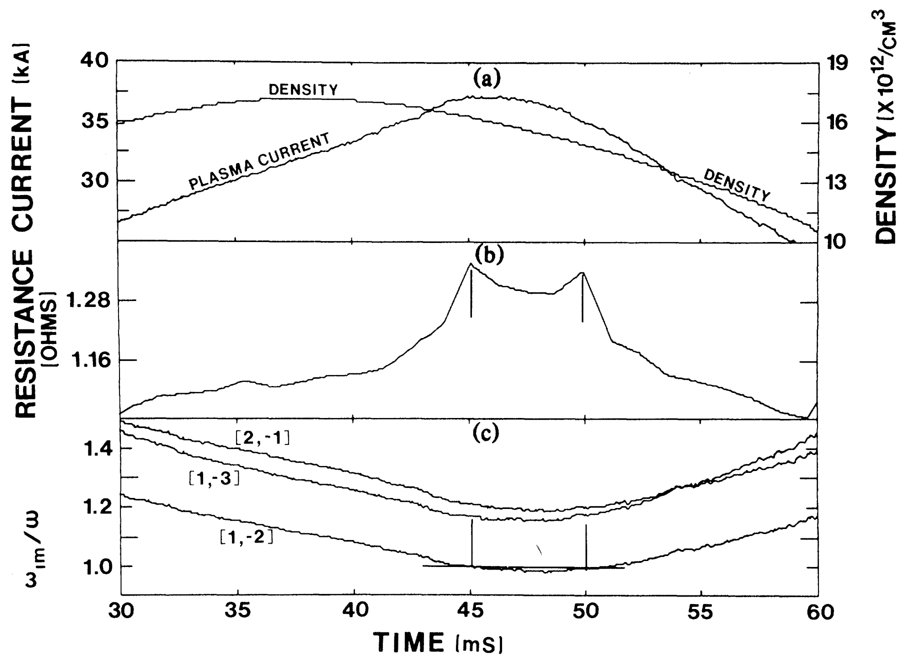

FIG. 1. (a) Plasma current and density as a function of time. (b) Antenna resistance for a single antenna. (c) ω_{lm}/ω a function of time for mode numbers $(l,m) = (2, -1)$, $(1, -3)$, and $(1, -2)$; $m_{\text{eff}} = 1.5$.

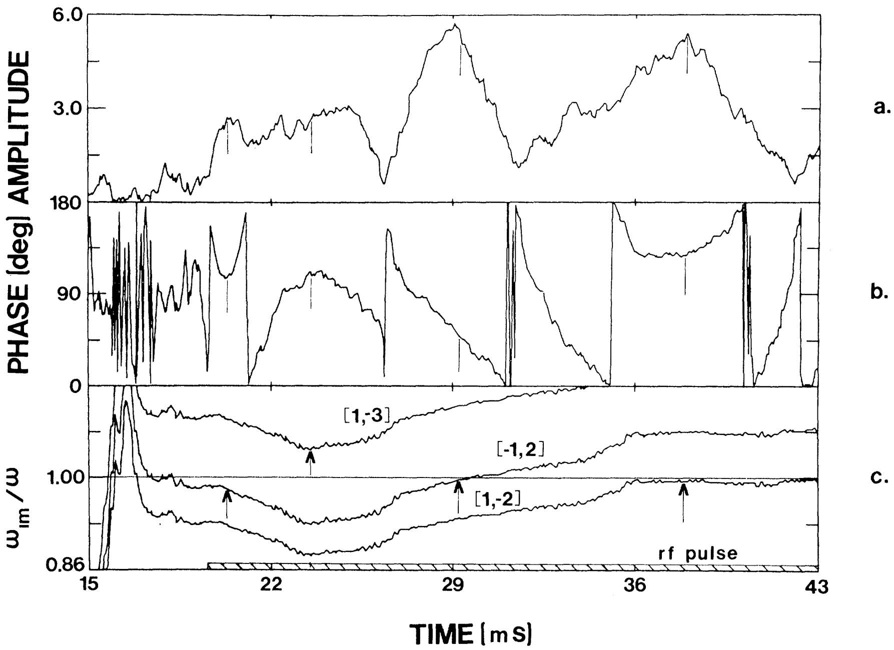

FIG. 2. (a) Amplitude of the interferometer signal as a function of time. (b) Phase change of the interferometer signal relative to the antenna current as a function of time. (c) ω_{lm}/ω as a function of time for mode numbers $(l,m)=(1,-3)$, $(-1,2)$, and $(1,-2)$; $m_{\text{eff}}=2.07$. The rf pulse, which begins at 19 ms, is denoted with crosshatching.

Note that the calculated frequency scales with $m_{\text{eff}}^{-1/2}$, which is not directly measured. Measurements[14] of Z_{eff} using earlier Thomson-scattering temperature profiles have shown a range $2.5 \leqslant Z_{\text{eff}} \leqslant 5$ under typical operating conditions. With the assumption that the dominant state of ionization is five or six times ionized oxygen, we can restrict the range of effective mass to $1.5 \leqslant m_{\text{eff}} \leqslant 2.2$. There are additional uncertainties of about $\pm 5\%$ in the calculation of ω_{lm} as regards the exact density and plasma current profiles. We assume a standard parabolic density profile which is consistent with measurements, and $q(r)=1+(q_a-1)r^2/a^2$, where q_a is the value of q at the limiter.

We have observed that, for similar plasma conditions, strongly peaked signals occur only when the two antenna currents are 180° out of phase, which implies that odd-l modes are being driven. Each signal peak observed can then be uniquely assigned a toroidal and poloidal mode number while satisfying $1.5 \leqslant m_{\text{eff}} \leqslant 2.2$. Figure 1(b) shows two peaks in the antenna resistance at 45 and 50 ms during a time when the plasma parameters are varying smoothly. We identify each peak as the $l=1$, $m=-2$ mode with $m_{\text{eff}}=1.5$. The increased loading resistance measured during this time is 0.2 ± 0.1 Ω, which is comparable to the 0.13 Ω calculated with the kinetic code of Ross, Chen, and Mahajan.[2,6]

Similar mode-identification techniques are used when analyzing the interferometer signal. Figures 2(a) and 2(b) show the time-dependent structure of the interferometer signal amplitude and phase relative to the antenna current. Figure 2(c) is a plot of ω_{lm}/ω for $l=\pm 1, m=\mp 2$ and $l=1, m=-3$ with $m_{\text{eff}}=2.07$. By definition, a phase change of 180° is necessary for a complete sweep of the resonant frequency ω_{lm} through a mode. This is exemplified by the resonant peak shown between 26.5 and 31 ms. Figure 2 demonstrates the connection of our detected mode amplitude and phase with the calculated resonant frequencies for three modes. At 19 ms the rf is pulsed on while the $(-1,2)$ resonance approaches ω (i.e., $\omega_{-1,2}\rightarrow\omega$) from below. By 20.5 ms the $(-1,2)$ resonance reverses and begins moving away from $\omega=\omega_{-1,2}$. The behavior of $\omega_{-1,2}/\omega$ is directly reflected in both the amplitude and the phase plots. The peak amplitude occurs at the point that $\omega_{-1,2}/\omega$ turns around which is also the point at which the mode phase reverses its direction. The same behavior occurs again as the $(1,-3)$ resonance approaches ω from above. After 23 ms there is a period over which the frequencies ω_{lm}/ω rise continuously. During this time the $(-1,2)$ resonant frequency approaches and crosses the driver frequency giving us a full resonance sweep centered at

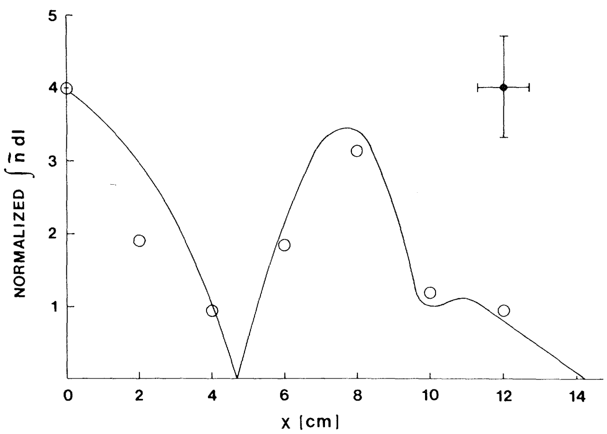

FIG. 3. An experimental and theoretical comparison of the amplitude of the density fluctuations using one toroidal antenna as a function of interferometer position.

29.5 ms. Finally at 38 ms the (1,−2) resonance approaches the driver and slowly turns around in a similar fashion to the first two resonances. Note that the splitting of the $(l,m) = (1, -2), (-1, 2)$ modes due to ω/ω_{ci} effects is demonstrated in Fig. 2 and there is agreement between Eq. (1) and the experiment.

Using the method described for Fig. 2 we identify the (1,−2) mode over many shots. We select only peaks which show a full 180° phase shift and plot the peak amplitude as a function of the distance between the laser chord and the center of the plasma. In Fig. 3, the solid line is a plot of the function $\int dy\, \tilde{n}(r) \exp(im\theta)|_x$ derived from the kinetic theory code for the fundamental radial eigenmode.[6] The zero at $r = 4.7$ cm is the result of chord averaging. The open circles represent experimental values of the interferometer signal amplitude. Each circle represents a mean value of 5–10 points for that position with theory and experiment normalized at $x = 0$ to facilitate a comparison. The calibrated laser interferometer amplitude at $x = 0$ with two antennas operated out of phase and a current of 180 A in each antenna is $[\int \tilde{n}\, dl]_{\text{exp}} = 2.5 \times 10^{11}$ cm^{-2} to within a factor of 2, while theory predicts an amplitude of $[\int \tilde{n}\, dl]_{\text{code}} = 7.2 \times 10^{11}$ cm^{-2} at this position.

The wave damping can be estimated by comparing the measured $Q = \omega/\Delta\omega \simeq 55 \pm 10$ and the predicted $\omega/\Delta\omega = \text{Re}\omega/\text{Im}\omega = 57$. This measurement was done at a power range of 1–10 kW. The close agreement between theory and experiment is strong support for the collisionless kinetic model of the plasma.

We have thus identified several global Alfvén eigenmodes and studied the amplitude structure and damping of the $(1, -2)$ mode using laser interferometry. The agreement with kinetic theory predictions is good. The detailed understanding of location and structure of the global modes may prove to be an important first step in our attempts to understand phenomena ranging from laboratory plasma heating to heating of solar coronas.

The authors would like to express their appreciation to S.-H. Lin, A. Hasegawa, and R. B. Michie for their advice and assistance. The work was supported by the U. S. Department of Energy under Contracts No. DE-AC05-78ET53043 and No. DE-AC05-76ET53036, The University of Texas, and the Texas Atomic Energy Research Foundation.

[1]Preliminary results were presented by R. D. Bengtson *et al.*, in Proceedings of the Fifth Topical Conference on Radio Frequency Plasma Heating, Madison, Wisconsin, 1983 (to be published), paper D2. See also T. E. Evans *et al.*, *ibid.*, paper CAl; M. E. Oakes *et al.*, *ibid.*, paper CA3.

[2]R. D. Bengtson *et al.*, in *Heating in Toroidal Plasmas III,* edited by C. Gormezano (Pergamon, New York, 1982), Vol. 1, p. 151.

[3]A. de Chambrier *et al.*, Plasma Phys. **24**, 893 (1982).

[4]J. P. Goedbloed, Phys. Fluids **18**, 1258 (1975).

[5]A. Pochelon *et al.*, in *Proceedings of the Seventh European Conference on Controlled Fusion and Plasma Physics, Lausanne, Switzerland, 1975* (European Physical Society, Geneva, 1975), Vol. 1, p. 157.

[6]D. W. Ross, G. L. Chen, and S. M. Mahajan, Phys. Fluids **25**, 652 (1962).

[7]K. Appert, R. Gruber, F. Troyon, and J. Vaclavik, in *Heating in Toroidal Plasmas III,* edited by C. Gormezano (Pergamon, New York, 1982), Vol. 1, p. 203.

[8]K. Appert, R. Gruber, F. Troyon, and J. Vaclavik, Plasma Phys. **24**, 1147 (1982).

[9]S. M. Mahajan and D. W. Ross, Phys. Fluids **26**, 2195 (1983).

[10]S. M. Mahajan, University of Texas Report No. IFSR 84, 1983 (to be published).

[11]K. Appert, J. Vaclavik, and L. Villard, Phys. Fluids **27**, 432 (1984).

[12]J. A. Tataronis and W. Grossmann, Nucl. Fusion **16**, 667 (1976).

[13]S.-H. Lin, M. E. Oakes, and R. D. Bengtson, IEEE Trans. Plasma Sci. **11**, 64 (1983).

[14]S. M. McCool, "Thomson Scattering on the PRETEXT Tokamak," Ph.D. Dissertation, The University of Texas at Austin, 1982 (unpublished).